

# **The Application of Electron Microscopy Techniques to the Space Shuttle Columbia Accident Investigation.**

Dr. Sandeep Shah and Greg Jerman  
Materials Diagnostics Team, NASA Marshall Space Flight Center  
[Sandeep.r.shah@nasa.gov](mailto:Sandeep.r.shah@nasa.gov), [Gregory.a.jerman@nasa.gov](mailto:Gregory.a.jerman@nasa.gov)

The Space Shuttle Columbia was returning from a 16-day research mission, STS-107, with nominal system performance prior to the beginning of the entry interface into earth's upper atmosphere. Approximately one minute and twenty four seconds into the peak heating region of the entry interface, an off-nominal temperature rise was observed in the left main landing gear brake line. Nearly seven minutes later, all contact was lost with Columbia. Debris was observed periodically exiting the Shuttle's flight path throughout the reentry profile over California, Nevada, and New Mexico, until its final breakup over Texas. During the subsequent investigation, electron microscopy techniques were crucial in revealing the location of the fatal damage that resulted in the loss of Columbia and her crew.

## **Beginning the Investigation**

After the loss of Columbia was confirmed, NASA immediately implemented procedures adopted as a result of the 1986 Challenger tragedy. An independent Columbia Accident Investigation Board (CAIB) was formed and assigned the responsibility of finding the root causes for the disaster. NASA teams were responsible for the recovery, identification, reconstruction, and analysis of the debris, but the recovered hardware belonged to the CAIB and analysis was directed solely by the CAIB. Columbia debris was collected, catalogued, and reassembled at the Shuttle Landing Facility (SLF) located on the Kennedy Space Center (KSC) during an intensive four-month period. Scattered over a vast length of Texas, 85,000 pieces of Columbia were recovered that represented 40 percent of the shuttle by weight. The Materials & Processes Failure Analysis Team was tasked with analysis of selected debris components. This team was challenged with collecting and interpreting physical evidence that could verify the sequence of events that led to the loss of Columbia and her crew, as seen in figure 1.

## **The Challenge**

Sensor spikes associated with the left main landing gear indicated the initial failure probably started in the left wing, but where do you begin the failure analysis of 85,000 pieces of evidence? What questions needed to be asked, and how many parts required analysis? What was the priority of each analysis? The final challenge that threatened to undermine basic evidence interpretation was distinguishing between damage that occurred before the shuttle disintegrated and damage that resulted from breakup, re-entry, and ground impacts. The Materials and Processes Failure Analysis Team was responsible for providing the CAIB with factual analytical evidence relating to the condition of debris items. Interpretation of the analytical evidence was kept separate so the CAIB could collect various opinions on the meaning of the raw data without fear of shading the basic facts. Initial non-destructive analysis began on several debris items based on visual inspection that was correlated with available flight sensor data. Items such as the main landing gear strut and tires, uplock rollers, midbody panels, thermal protection system tiles, and Wing Leading Edge (WLE) hardware were photographed and x-rayed in preparation for more extensive failure analysis activities. To better visualize the condition of debris items relative to each other and their location on the Shuttle, the wing, tail, and fuselage debris were laid out on a grid as seen in figure 2.

About six weeks after the crash, the fortunate recovery of more extensive sensor information from Columbia's on-board data recorder "black box" provided a clear sequence of sensor failures that significantly narrowed the possible locations of an initial breach. The timed sequence of sensor failures revealed the first off-nominal temperature increase started in the left WLE at a thermocouple located behind the U-shaped Reinforced Carbon-Carbon (RCC) panel 9. RCC is a high temperature carbon fiber/carbon matrix composite that is protected from oxidation by a silicon carbide coating. Although RCC is designed to operate at temperatures up

to 3000 °F, it is extremely brittle and will shatter like glass if overstressed. Because the thermocouple in the cavity behind left WLE RCC panel 9 was the first to fail, prior to any other sensors, the analysis of debris items focused on the left WLE RCC panels where launch video indicated foam from the external tank had impacted on ascent as seen in figure 3.

### **Left Wing Leading Edge**

There are 22 RCC panels protecting the leading edge of each wing from hot gasses during re-entry. The gap between each panel is sealed with a short T-shaped RCC seal. The arrangement of the wing leading edge is shown in Figure 4. The highest heating during re-entry occurs in panels 7-10, right where the wing leading edge surface changes direction. After recovery and identification, the reconstructed pieces of Columbia's RCC panels and T-seals were qualitatively examined for damage patterns. The internal surfaces of left wing RCC panels 7 through 10 showed heavy deposition of material that was best described by the metallurgical term slag. The deposits on the RCC panels were expected to originate from Columbia's metal wing structures. Some RCC panels from the right wing also contained slag deposits although to a lesser degree. Figure 5 shows one example of slag deposits on the inside surface of left wing RCC panel 8. There were other visual signs of significant heat damage including melted RCC attachment hardware and knife edge erosion on broken edges of RCC panels. Most of the slag deposits, molten RCC attachments, and eroded RCC were concentrated between RCC panels 7 through 10 on the left wing.

The key to deciphering the sequence of damage events was to understand the origins of the slag deposition. By understanding the composition of the materials in the WLE, it was hoped the origin of the slag deposits could be identified. The major WLE materials and components included RCC, 2024 aluminum wing spar, A286 steel attachment fittings, Inconel 718 spanner beams and bolts, 6061 aluminum carrier panels, Inconel 601 foil around flexible cerachrome insulation, Inconel 625 insulation attachment clips, and silica thermal protection tiles. Figure 6 shows a cross-section of the WLE including material identification. Slag specimens were extracted from many RCC panels from both the left and right WLE with the underlying RCC intact and quantitatively analyzed to determine their chemistry and morphology.

### **Analysis Techniques, Plan and Interpretation Criteria**

Table 1 lists the techniques that were considered for slag analysis. Several practice samples were used to test these techniques and determine the level of information that could be obtained. After the trial evaluations, a few techniques were found to be acceptable for the final production analysis of RCC slag samples cut from left wing RCC panels 7, 8, 9, and 10 and right wing RCC panel 8. Repeatability and reproducibility were emphasized through multiple sampling of similar features and through analysis by multiple techniques. Similar results quantitatively and qualitatively reproduced by different techniques allowed for cross checking of results which minimized the possibility of analytical error.

The final analysis techniques included radiography to see through the RCC slag deposits and identify unique features. Scanning Electron Microscopy (SEM), Energy Dispersive x-ray Spectroscopy (EDS), elemental x-ray dot mapping, and backscattered electron imaging of slag cross sections were used to identify elements and their physical microstructural distribution. Electron microprobe performed accurate quantitative chemistry of microstructural features identified in the SEM. X-ray diffraction and Electron Spectroscopy for Chemical Analysis (ESCA) provided quantitative compound information that complemented the chemistry determined by electron microprobe.

Interpretation criteria were necessary to identify the origin of localized WLE slag deposits. The high temperature structural WLE alloys Inconel 601, Inconel 718, Inconel 625, and A286, all contained nickel and iron as their major constituents. The ratio of nickel to iron atomic percentages provided the most reliable finger print of each alloy. The presence or absence of minor alloying elements such as molybdenum, niobium, cobalt, and titanium were also used in conjunction with Ni/Fe ratio. Cerachrome insulation, used to shield the aluminum wing spar from heating, was identified by its unique green color and its composition that contained mostly silica, alumina, and some chromium oxide. Thermal protection tiles were composed of pure silica that

made them easily identifiable. The wing spar was manufactured from 2024 aluminum which contains copper as a strengthening additive.

### **Analysis of Wing Leading Edge RCC Slag Deposits**

Dozens of RCC cross sections were analyzed for slag deposit chemistry and morphology generating approximately 2000 pages of chemical and morphological data. One sample analysis from the left wing RCC panel 8 is presented here to exemplify the process. In this case, unique metallic spheroids were found that were in direct contact with RCC surface as seen in Figure 7. Like a layered cake, the first slag deposits represented the first damage event, while the outer slag surface represented the last damage event. SEM x-ray dot maps in Figure 8 shows high concentrations of iron, nickel, and chromium in these spheroids. Backscattered imaging clearly showed metallic deposits versus oxide type deposits in the vicinity of the spheres. Quantitative electron microprobe results identified spheroid compositions that closely matched Inconel 718 and Inconel 601 which correspond to the metallic RCC attachment hardware and the internal insulation foil. The final layers on top of the spheroids contained oxidized and metallic aluminum with copper that uniquely identified the 2024 wing spar as the source for the final deposits as seen in figure 9.

Similar layering information was obtained for slag deposits on both the left and right wing RCC panels. Physical features such as tear shaped deposits, globular deposits, and uniform slag layering were analyzed. Correlation of the slag analysis revealed the pattern and timing of thermal damage:

1. In left wing RCC pieces, cerachrome insulation and Inconel 718 or Inconel 601 primarily made up the first deposited slag layer. This suggests the first damage occurred by melting of RCC attachment beams and internal insulation.
2. In left wing RCC pieces, aluminum deposition was secondary suggesting the wing spar melted last.
3. In left wing RCC pieces, there was no indication of A286 wing spar attachment fittings in the first slag deposits suggesting the initial plasma impingement was through a breach near the RCC attachment points and not near the wing spar.
4. In left wing RCC pieces, there is large amount of molten ceramic cerachrome insulation on the inside of RCC panels suggesting temperatures were in excess of 3200 °F.
5. Left wing slag distribution and shape identified the plasma flow direction and the deposition thickness inferred a long duration.
6. Right wing slag deposits were thin and uniform including simultaneous deposition of cerachrome, aluminum, and Inconel materials that implied all components were melting together during breakup.

### **Analysis of Slag Deposits on Thermal Protection Tiles**

Many of the thermal protection tiles immediately behind the WLE RCC panels were recovered and radiographed. They did not show any evidence of embedded material, but their surfaces did have discoloration and localized melting. The directionality of the discoloration and melting indicated hot plasma was exiting from the top corner of RCC panel 8 onto the tiles behind RCC panel 9. Cross sections of the discolored and melted tiles were analyzed in the SEM and electron microprobe. Like the internal RCC slag deposits, the thermal tile discoloration contained layers of material that were chemically consistent with the internal WLE structures.

### **Breach Scenario from Analysis Results**

After correlating all analyses, a scenario for the progression of damage in Columbia's wing is depicted in Figure 10. The breach started on the underside of the left wing at RCC panel 8, close to the T-seal between panels 8 and 9. The plasma first impinged on the Inconel 718 attachments that held the RCC in place and insulation that protected the aluminum wing spar from overheating. The flexible insulation was not designed to contain hot flowing plasma which continued to circulate around inside the left wing at RCC panel 8 creating molten cerachrome tears and droplets. Eventually the insulation failed between panels 7 and 9 allowing plasma to move downstream and upstream from panel 8. Eventually the lower RCC attachment points for panels 8 and 9 collapsed causing massive plasma impingement on the aluminum wing spar at temperatures greater than 3200 °F.

The final failure scenario generated from the analytical data identified the initial breach location as the same as visual observations, and area where foam from the external tank had impacted the wing leading edge on ascent. Had the breach occurred away from the hottest RCC panels between 7 and 10 on the WLE, Columbia may have survived the peak heating of re-entry structurally intact. They were only a minute away from the end of peak heating.

### Acknowledgements

The authors would like to acknowledge the significant analytical and interpretive contributions of material scientists and failure analysts from the Kennedy Space Center, Johnson Space Center, Glenn Research Center, Langley Research Center, White Sands Test Facility, United Space Alliance, Boeing and the Columbia Accident Investigation Board.



Figure 1. Astronauts of Space Shuttle Columbia, Columbia on launch pad, and liftoff.

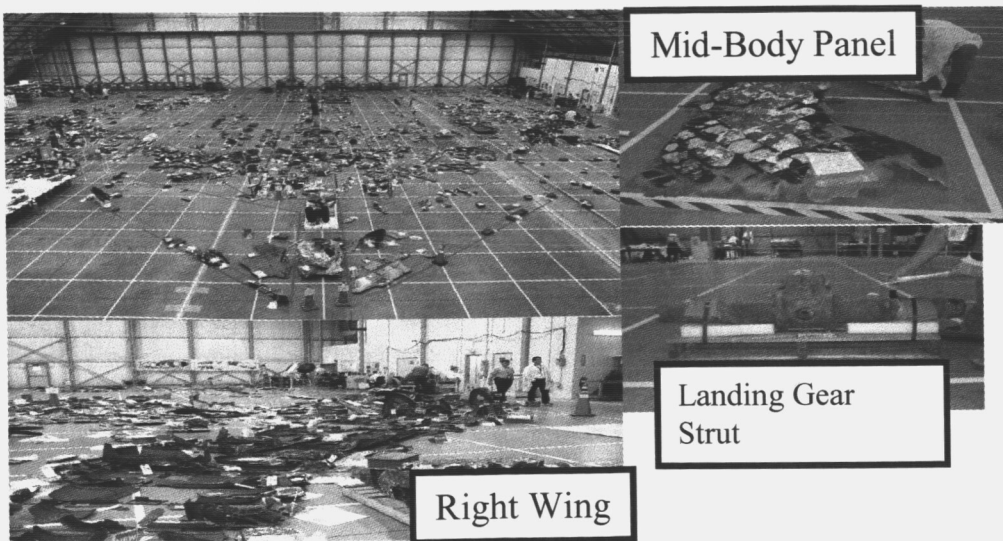


Figure 2: Hardware recovered, identified, and laid in a grid pattern at shuttle's landing facility.

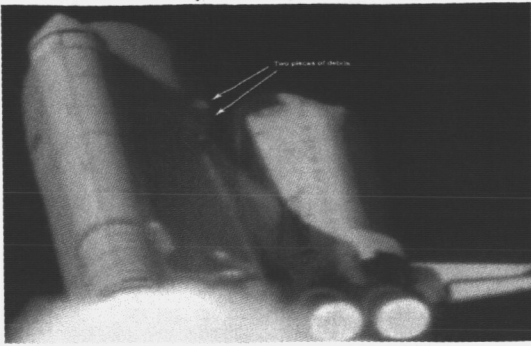


Figure 3: Evidence of foam hitting the shuttle's left wing.

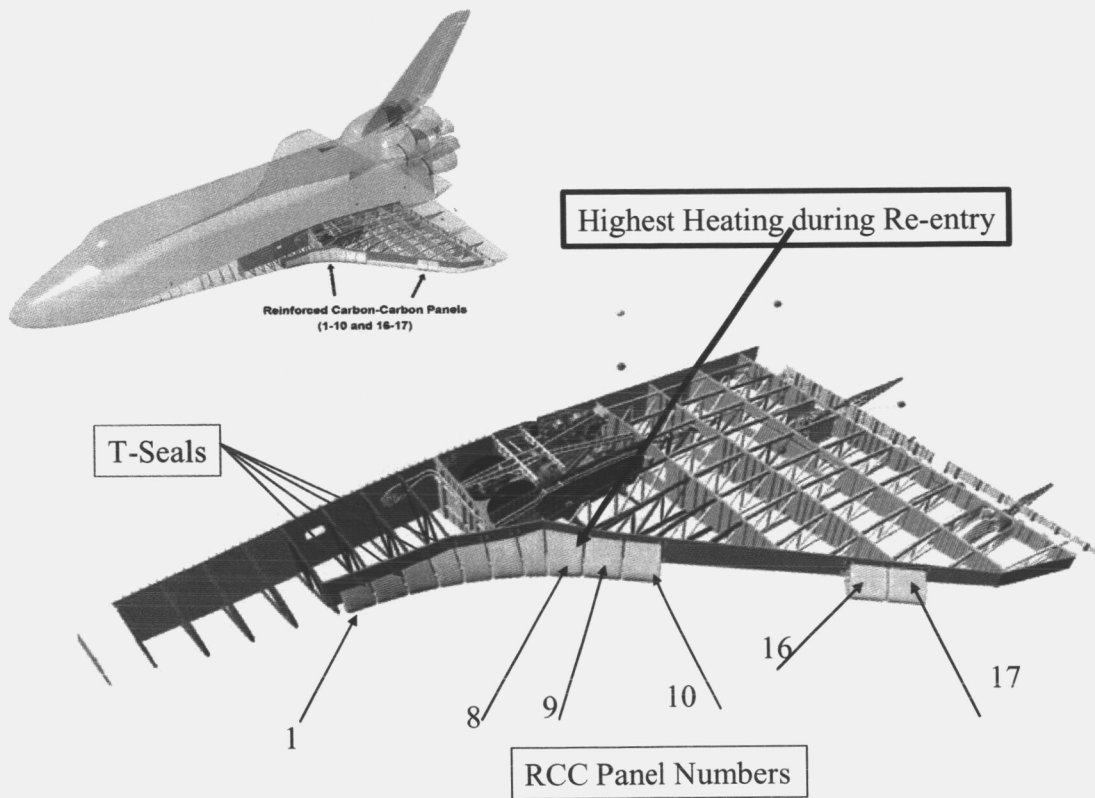


Figure 4: Arrangement of 22 RCC panels and T-seals on the wing leading edge.



Figure 5: Left wing RCC panel 8 with slag deposit on the inside.

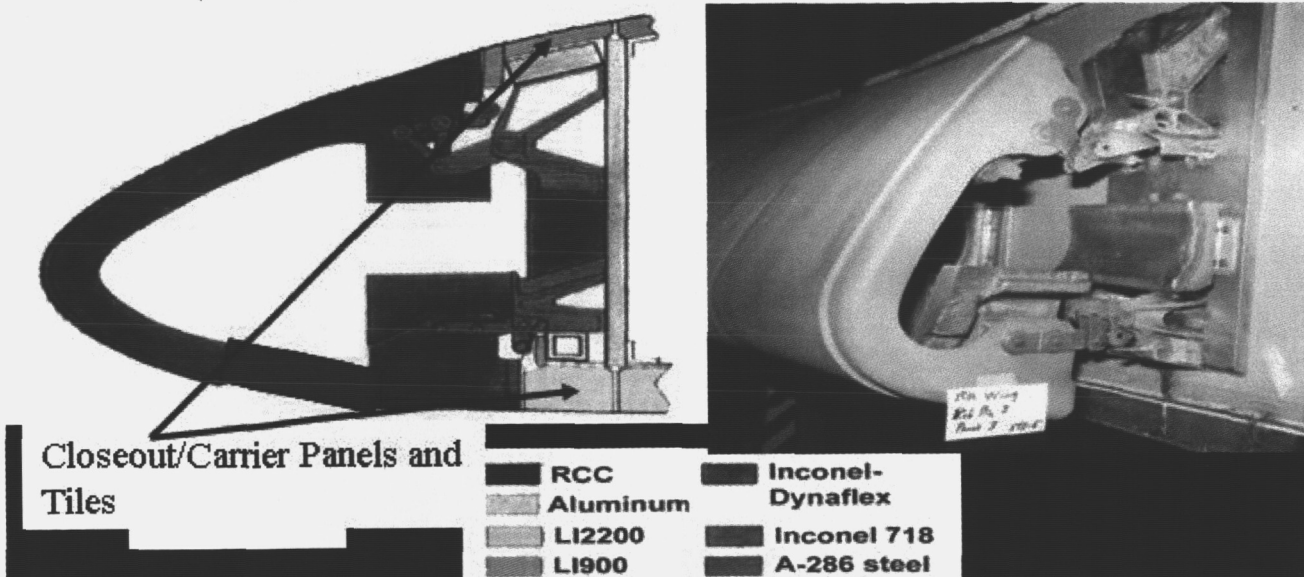


Figure 6: Cross-section through the wing leading edge including major component materials.

Analysis Technique	Purpose	Why/Advantages
Photography	Photo documentation	Documentation to maintain traceability
Scanning Electron Microscopy – SEM/EDS	Semi-quant elemental composition Back Scattered Imaging	Elements present, identify difference between top and bottom, X-ray mapping.
X-ray Diffraction - XRD	Identify compounds	Identify compounds of crystalline structure
Electron Microprobe	Identify elements	Determine exact composition
Fourier Transform Infra-Red	Qualitative organic comp.	If organic, aid in identification
ESCA/XPS	Identify inorganic & organic compounds	Aid in tracking of oxidation states, such as oxide; compound identification
Metallography + SEM	Layering of material	Composition through deposit layers
Inductively coupled plasma - ICP	Quantitative elemental composition	Elements present, Quantify bulk composition of sample
Radiography, CT, Ultrasonics	NDI and identification	See through the material, identify differences in materials, identify defects

Table 1: List of available analysis techniques with high reliability and reproducibility.

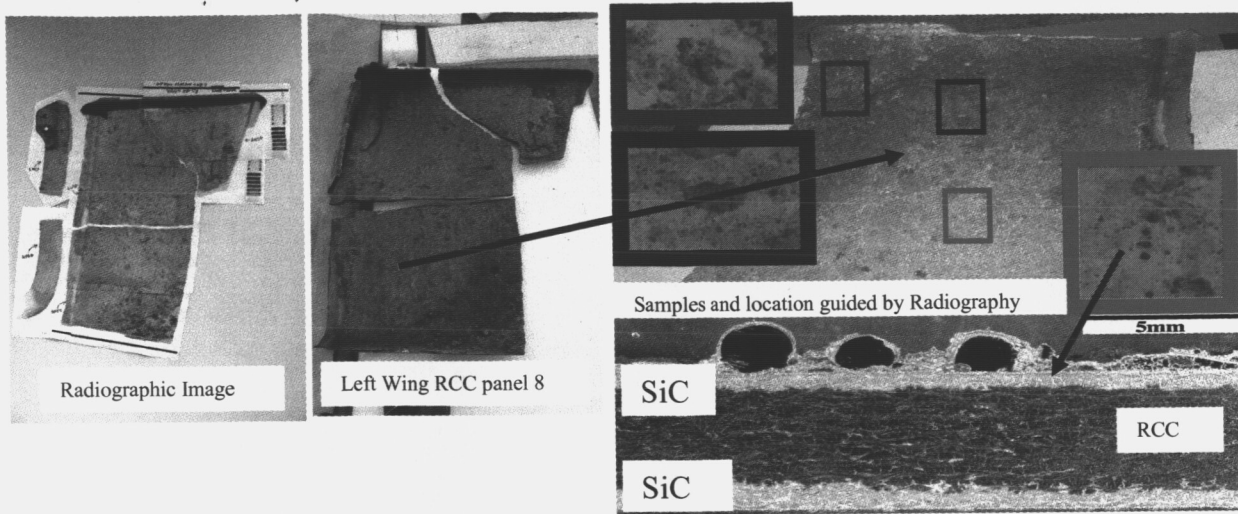


Figure 7: Cross-section through unique spheroids in slag deposits on the left WLE RCC panel 8.

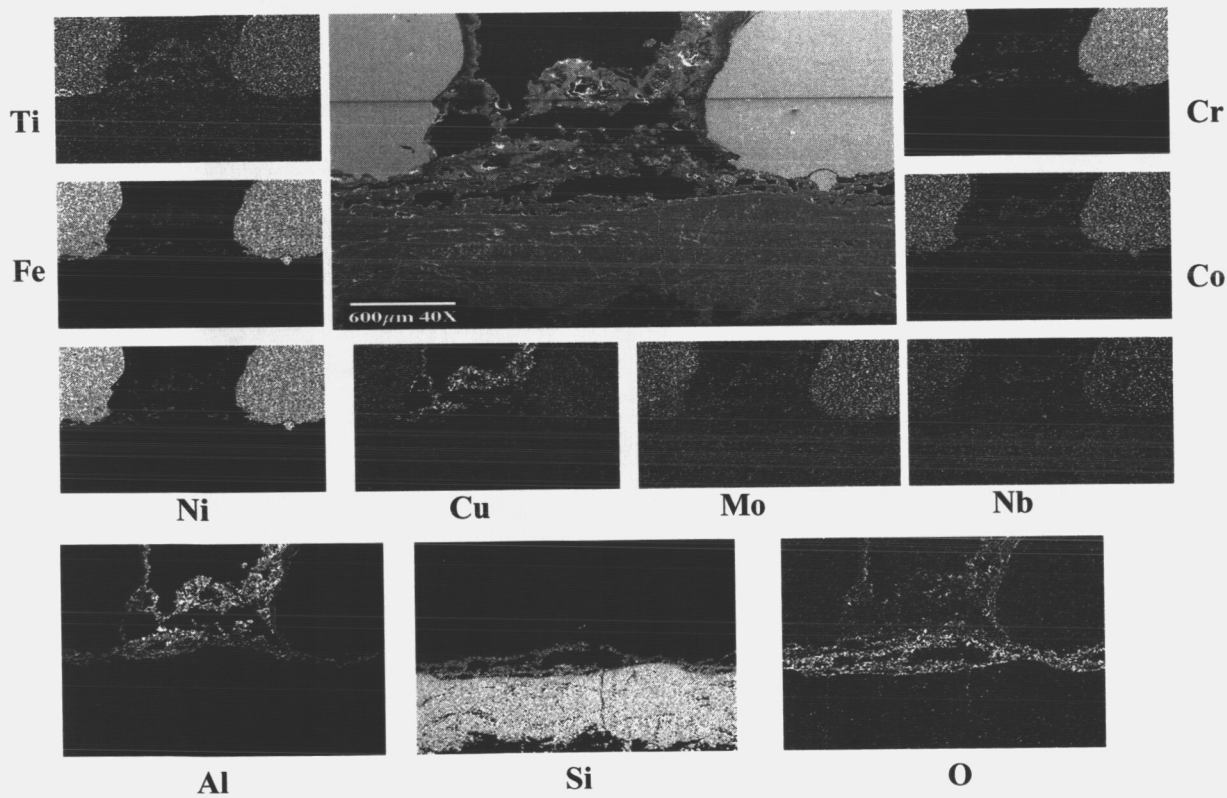


Figure 8: X-ray map showing distribution of various elements in and around spheroids of Figure 6.

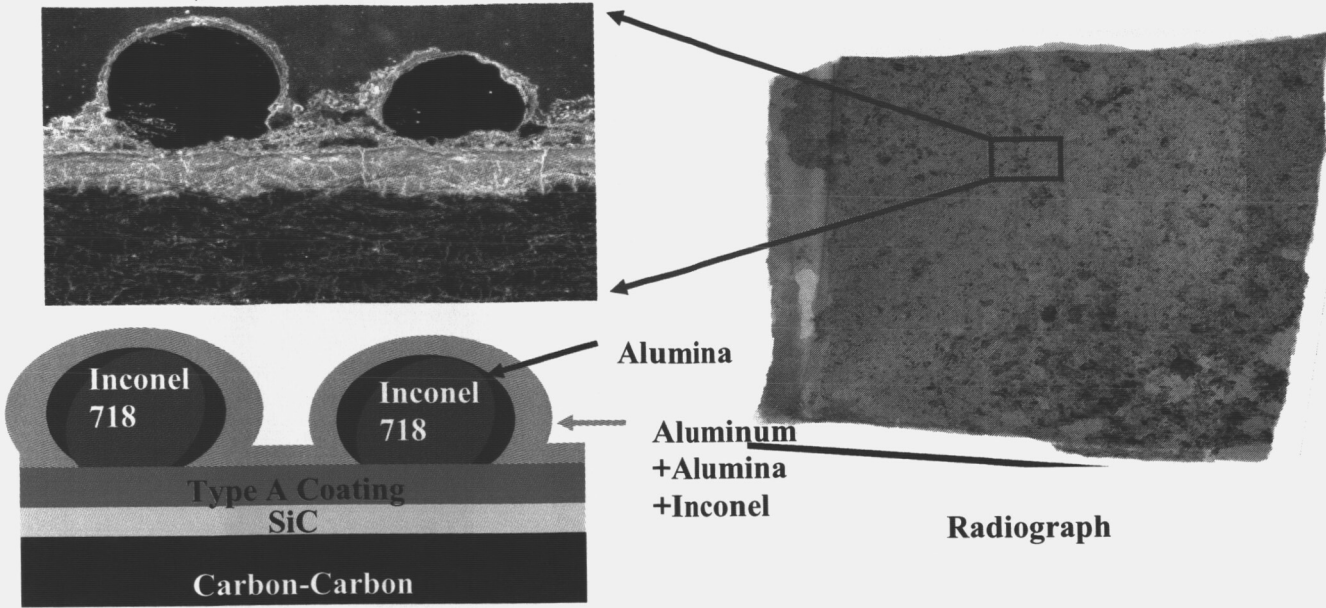


Figure 9: Layering of slag showing sequence of damage and deposition events.

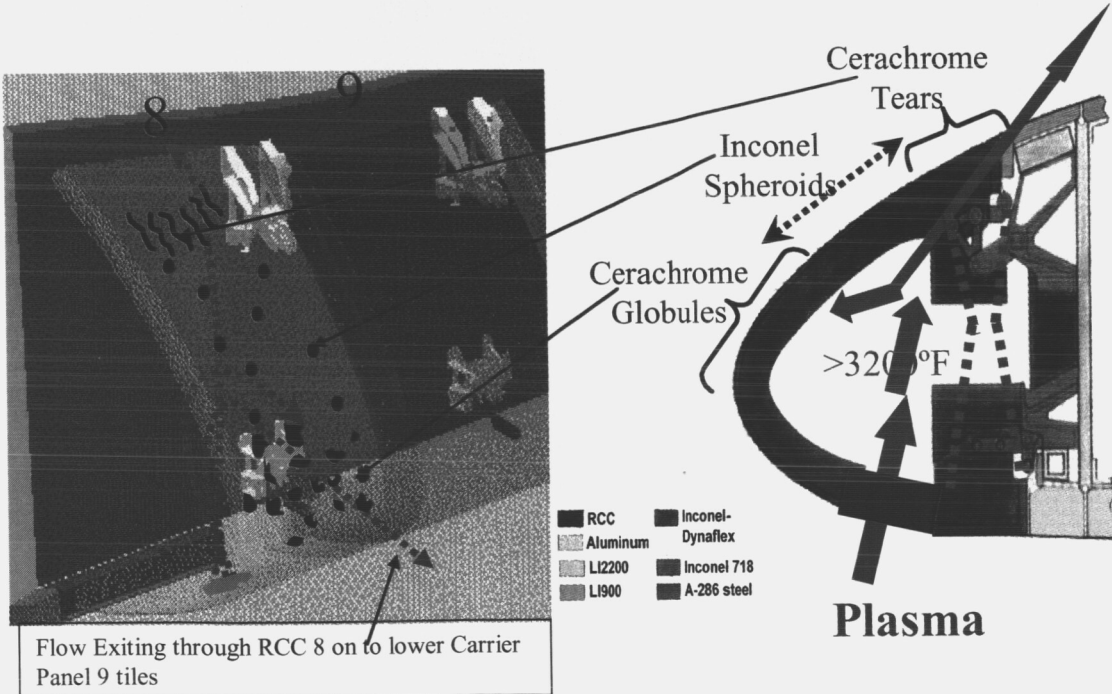


Figure 10: Breach scenario and location based on analysis results.